RSC Advances

ROYAL SOCIETY OF CHEMISTRY

www.rsc.org/advances

1 Umbelliprenin and Lariciresinol isolated from a long-term-used

2 herb medicine *Ferula sinkiangensis* induce apoptosis and G0/G1

3 arresting in gastric cancer cells

4

5

6 Lijing Zhang[a], Jianyong Si[a], Guangzhi Li[a], Xiaojin Li[b], Leilei Zhang[a], Li

7 Gao[a], Xiaowei Huo[a], Dongyu Liu[a], Xiaobo Sun[a], Li Cao[a]*

8

9 *[a] Institute of Medicinal Plant Development, Chinese Academy of Medical*

10 *Sciences & Peking Union Medical College, Beijing, China*

11 *b Xinjiang Institute of Chinese Materia Medica and Ethnodrug, Urumqi,*

12 *Xinjiang Province 830002, China*

13

14 Corresponding author

15 Prof. Li Cao

16 E-mail address: lcao@implad.ac.cn.

17 Tel.: +86-010-57833222;

18 Fax: +86-010-57833222

19 Postal address: 151# Malianwa North Road, Haidian District, Beijing

20 100193, China.

21 **Abstract**

22 Effective chemicals isolated from folk medicine are commonly used

23 in the treatment of cancer in Asian countries like China and India.

24 *Ferula sinkiangensis* K. M. Shen is a traditional herb medicine used

25 for treating stomach disorders in Xinjiang District of China for

26 thousands of years. Here, we showed that the growth inhibition effects

27 of seven compounds first isolated from the seeds of this herb in human

28 gastric cancer cells and human normal gastric epithelium cells.

29 Furthermore, we characterized the mechanism of the antiproliferation

30 effects on gastric cancer cells of the two most specific and effective

31 compounds: Umbelliprenin (UM) and Lariciresinol (LA). Annexin V/PI

32 staining demonstrated that UM and LA induce apoptosis in gastric cancer

33 AGS cells. Loss of mitochondrial membrane potential, upregulation of

34 proapoptotic protein BAX, and activation of Caspase 3 and PARP

35 suggested that UM and LA caused the activation of the mitochondrial

36 apoptosis pathway. Cell cycle analysis showed that UM and LA arrest cell

37 cycle at G0/G1 phase. Western blot results showed that the expression of

38 P53, P27, P16 and Rb proteins increased, while the expression of Cyclin

39 D, Cyclin E, Cdk4 and Cdk2 decreased in cancer cells. Overall, these data

40 provided evidence that UM and LA have the potential to be used in

41 cancer therapy.

42

43 **Introduction**

44 Gastric cancer is characterized by high mortality rates, and one of the

45 most common malignant cancers worldwide [1]. The median survival of

46 patients with this metastatic disease is less than one year [2]. The current

47 treatment therapy for gastric cancer is chemotherapy, but because the side

48 effects are severe, its application is limited, and effective agents are

49 urgently needed to improve the prognoses of patients. Although several

50 agents are under clinical evaluation for gastric cancer such as trastuzumab

51 and cetuximab [3,4], the effective response rate of gastric cancer patients to

52 these treatments is low (only 30-40%) [5]. Recently, natural products for

53 gastric cancer treatment therapy have obtained increasing attention [6,7]. _F._

54 _sinkiangensis_ was originally described in the "Medica of the Tang

55 Dynasty". As a traditional folk medicine used for the treatment of

56 stomach disorders in Xinjiang District of China for thousands of years,

57 the potential value of this herb for treating gastric cancer could not be

58 ignored [8]. Although there have been studies on the chemical composition

59 and anti-inflammation activity of this herb [9,10], the effective components

60 and mechanism in gastric cancer treatment are still not clear. Our

61 previous studies have found that a petroleum ether extract of the seeds

62 showed antitumor activity (Unpublished data). Many compounds,

63 including steroidal esters and lignin, have been isolated from the seeds

64 [11,12]. In the present study, we first screened these compounds for the

65 growth inhibition effect in gastric cancer cells, and then characterized the

66 possible mechanism. We found that UM and LA were the two most

67 cytotoxic compounds towards gastric cancer cells, and the least cytotoxic

68 to normal gastric epithelial cells, compared with other compounds. In

69 addition, the two compounds induced apoptosis and cell cycle arrest in

70 gastric cancer cells.

71 **Materials and Methods**

72 **Plant material**

73 The seeds of *F. sinkiangensis* were collected from Yili state, Xinjiang

74 Uygur Autonomous Region of China, in July 2008, and were identified

75 by Professor Xiaojin Li. A voucher specimen (No. AP21020720) was

76 deposited in the Xinjiang Institute of Chinese Materia Medica and

77 Ethnodrug.

78 **Test compounds**

79 The seeds of *F. sinkiangensis* were crushed and refluxed with 95% EtOH

80 for three times, 2 h for each extraction. Then combined the EtOH extracts,

81 evaporated under reduced pressure to yield residue, suspended in water

82 and then partitioned using petroleum ether and dichloromethane. The

83 dichloromethane extract was further fractionated into ten fractions (A-J)

84 using silica gel chromatography with $CHCl_3$–MeOH (40:1 to 0:1, v/v).

85 Fraction B was subjected to silica gel column chromatography using a

86 Sephadex LH-20 column (2.5 × 150 cm) eluting with MeOH, and ten

87 fractions were obtained. Fraction B-4 and Fraction B-6 were purified by

88 semi-preparative HPLC to obtain compound 1 (tR = 19 min), compound

89   2 (tR = 21 min); Fraction B-9 was subjected to silica gel column

90   chromatography eluting with CHCl3–MeOH (20:1 to 0:1, v/v), and 12

91   fractions were obtain (Fraction B-9-1--B-9-12). Fraction B-9-4 was

92   eluted with $CHCl_3$–MeOH–H_2O (7.5:2.5:1) by preparative scale

93   chromatography and compound 3 was obtained (Rf =0.6). Then using a

94   MeOH–H_2O (47:53) system to obtain compound 4 (tR 23 min) and

95   compound 5 (tR 33 min) from Fraction B-9-7. Finally, a MeOH–H2O

96   (52:48) system was used to obtain compound 6 (tR 33.7 min) and

97   compound 7 (tR 37.6 min) from Fraction B-9-11. These compounds were

98   identified by spectra methods (UV, IR, MS and NMR) and purified by

99   HPLC (purity > 90%). And compound 1 to compounds 7 were

100   (7,8-cis-8,8'-trans)-2-4-dihydroxyl-3,5-dimethoxy-lariciresinol($C_{20}H_{24}O_6$),

101   Lehmannolol ($C_{24}H_{32}O_4$), Arctigenin ($C_{21}H_{24}O_6$), Quercetin ($C_{15}H_{10}O_7$),

102   Macrathoin F ($C_{26}H_{26}O_{12}$), Umbelliprenin ($C_{24}H_{30}O_3$), and Lariciresinol

103   ($C_{20}H_{24}O_6$). The chromatographic profiles of UM and LA are shown in

104   supplemental information. These compounds were dissolved as stock

105   solutions in dimethyl sulfoxide (DMSO) and subjected to serial dilution

106   with medium before use so the final concentration of DMSO was less

107   than 1% (v/v).

108   **Reagents and antibodies**

109   Dulbecco's Modified Eagle's Medium (DMEM), Ham's F12 medium,

110   trypsin, penicillin, streptomycin, fetal bovine serum (FBS) were

111   purchased from Gibco (CA, USA), and 3-(4,5-dimethylthiazol-2-yl)-2,

112   5-diphenyltetrazolium bromide (MTT), DCFH-DA, DMSO, Hoechst

113   33342, 5,5′,6,6′-tetrachloro-1,1′,3,3′-tetraethyl-imidacarbocyanine iodide

114   (JC-1), RNase A, propidium iodide (PI) and trypan blue were purchased

115   from Sigma-Aldrich (MO, USA). The annexin V-FITC apoptosis

116   detection kit was obtained from KeyGEN Biotech (Jiangsu, China).

117   Antibodies against Bax, Bcl-2, Cleaved PARP, Cleaved Caspase-3,

118   Cyclin D1, Cyclin E, Cdk4, Cdk2, P16 and P27 were purchased from

119   Santa Cruz Biotechnology (CA, USA). Antibodies against Rb and β-actin

120   were obtained from Cell Signaling Technology (MA, USA). The cECL

121   Western Blot Kit was obtained from CoWin Biotech (Beijing, China). All

122   the chemical reagents were of the highest grade.

123

124   **Cell culture**

125   The human gastric carcinoma cell line AGS and the human prostate

126   carcinoma cell line PC3 were cultured in Ham's F12 medium containing

127   10% FBS, 100 U/mL penicillin, and 100 μg/mL streptomycin at 37°C

128   with 5% CO_2. The human normal gastric epithelial cell line GES-1,

129   human gastric cancer cell line BGC-823, human cervical carcinoma cell

130   line HeLa and human lung cancer cell line A549 were cultured in DMEM

131   supplemented with 10% FBS, 100 U/mL penicillin and 100 μg/mL

132   streptomycin under the same conditions. Cells were passaged at least

133   three times before being used in experiments.

134

Animals

136   Five-week-old male BALB/c nude mice were purchased from Vital River

137   Laboratories (Beijing, China) and maintained on a 12 h light/dark cycle

138   in a regulated environment ($25 \pm 2°C$), with free access to water and food.

139   The animal protocol was approved by the Animal Ethics Committee at

140   the Institute of Medicinal Plant Development, Chinese Academy of

141   Medical Sciences.

142

Cell viability and cytotoxicity assays

144   MTT assay was used to determine cell viability. Cells were seeded in

145   triplicate in 96-well plates and cultured at 37°C for 24 h. The cells were

146   treated with compounds in various concentrations (DMSO, 6.25, 12.5, 25,

147   50, 100 μM). After 24 or 48 h treatment, 10 μL MTT was added (5

148   mg/mL) to each well and incubated for another 4 h. The medium was

149   then removed and 150 μL DMSO was added. The absorbance was

150   measured at 570 nm using a Microplate Reader (Bio Tek, USA). Cell

151   viability was expressed as the ratio of surviving cells in each group to

152   cells in control group.

153   Trypan blue exclusion was used to examine the number of dead cells in

154   each group. AGS cells and GES-1 cells were plated in 24-well plates for

155   24 h and then treated with UM or LA (DMSO, 6.25, 12.5, 25, 50, 100 μM)

156   for 24 h. After harvesting, the cells were suspended in phosphate-buffered

157   saline (PBS) and mixed with 0.4% trypan blue dye solution. The numbers

158   of viable cells and dead cells were counted using light microscope.

159

Hoechst 33342 and AO/EB Staining

160

161   AGS cells were cultured in 96-well plates and treated with UM (0, 13.67,

162   27.34, 54.58 μM) or LA (0, 20.82, 41.62, 83.24 μM) for 24 h. After

163   washing with PBS, cells were stained with Hoechst 33342 for 20 min or

164   stained for 5 min with AO/EB. Nuclear morphology changes were

165   observed using Image Xpress Micro imaging system (Molecular Devices,

166   USA).

167

Apoptosis analysis

168

169   UM and LA induced apoptosis in AGS cells were detected using Annexin

170   V-FITC/PI apoptosis staining by flow cytometry. Cells were plated and

171   treated with UM (0, 13.67, 27.34, 54.58 μM) or LA (0, 20.82, 41.62,

172   83.24 μM) for 24 h. After harvesting and washing twice with cold PBS,

173   the cells were incubated with Annexin V and PI in binding buffer at room

174   temperature for 30 min in the dark. Stained cells were detected and

175   analyzed using FACS Calibur flow cytometry (Becton Dickinson, USA)

176   [28]. Apoptotic rates were reported as the percentage of apoptotic cells

177   among total cells.

178

Detection of Reactive Oxygen Species

180   ROS production was evaluated by the level of hydrogen peroxide

181   produced using DCFH-DA by flow cytometry. AGS cells were seeded in

182   6-well plates and treated with UM (0, 13.67, 27.34, 54.58 μM) or LA (0,

183   20.82, 41.62, 83.24 μM) for 24 h. The cells were then harvested and

184   incubated with 10 μM of DCFH-DA in serum-free medium for 30 min in

185   the dark at 37°C. After washing twice with cold PBS, the cells were

186   analyzed by FACS Calibur flow cytometry to measure ROS levels.

187

Mitochondrial membrane potential measurements (ΔΨm)

189   Changes in mitochondrial membrane potential after treatments were

190   measured by flow cytometry and Image Xpress Micro imaging system

191   (Molecular Devices, USA) using JC-1. Cells (1×10^6) were treated with

192   UM (0, 13.67, 27.34, 54.58 μM) or LA (0, 20.82, 41.62, 83.24 μM) for 24

193   h. Cells were then harvested and incubated with JC-1(5 μM) for 30 min in

194   the dark at 37 °C. After washing twice with PBS, the cells were analyzed

195   by flow cytometry and observed using Image Xpress Micro imaging

196   system.

197

Cell cycle analysis

199 Cell cycle distribution was measured by staining DNA with PI. Cells

200 (1×10^6) were seeded in 6-well plates and treated with UM (0, 13.67,

201 27.34, 54.58 μM) or LA (0, 20.82, 41.62, 83.24 μM) for 24 h. Then cells

202 were harvested and fixed with 70% ethanol overnight at -20 °C. After

203 washing twice with PBS, the cells were treated with RNase A for 20 min

204 and then stained with PI (50 mg/L) for 10 min in the dark [29] at room

205 temperature. The distribution of each phase in the cell cycle measured by

206 DNA content was detected using FACS Calibur flow cytometry and

207 analyzed by ModFit LT 4.0 software.

208

209 **Western blot**

210 AGS cells were exposed to UM (0, 13.67, 27.34, 54.58 μM) or LA (0,

211 20.82, 41.62, 83.24 μM) for 24 h. After collection, cells were lysed in

212 lysis buffer and protein concentrations were determined by the BCA

213 method. Protein samples were separated by SDS-PAGE and electrically

214 transferred onto PVDF membranes. After blocking with 5% non-fat milk

215 solution for 1 h, the membranes were incubated with primary antibody at

216 4°C overnight. Later, the primary antibody was washed with TBST and

217 incubated with secondary antibody at room temperature for 1 h. Protein

218 bands were visualized by ECL and the levels of β-actin for each sample

219 were used as a normalizing control.

220

221 **Effects of UM and LA in tumor xenograft models.**

222 Mice were inoculated subcutaneously with 1.0×10^6 BGC-823 human

223 gastric cancer cells on the right flank. The mice were randomized to six

224 groups of 8 mice per group the next day. Tumor growth was monitored

225 and tumor size was measured every day. When the tumor volume reached

226 approximately 0.3 mm in diameter, drug administration was initiated. UM

227 and LA were diluted in 0.9% NaCl to the final concentration of 10 mg/kg

228 or 20 mg/kg in 200 μL solution and administered to each mouse. UM and

229 LA solutions were administered twice a day for 12 days. Mice were then

230 euthanized and tumors were excised and weighed. Tumor inhibition rate

231 = (average weight of control group – average weight of treated group) /

232 average weight of control group× 100%.

233

234 **Statistical analysis**

235 All data were analyzed by software using IBM SPSS statistics 19.

236 Statistical significance between groups was defined as $*p < 0.05$ and $**p$

237 < 0.01.   Results were expressed as mean $\pm$ SD.

238

239 **Results**

240 **UM and LA preferentially inhibit the growth and induce the death of**

241 **human gastric cancer AGS cells.**

242 First we studied the anti-proliferative effects of seven compounds isolated

243   from the seeds of *F. sinkiangensis* (**Fig. 1a**) against four human

244   commonly observed cancer cell lines: stomach (AGS), cervix (HeLa),

245   lung (A549), prostate (PC3) cancer and human gastric epithelial cell line

246   GES-1. The concentrations resulting in 50% growth inhibition (IC_{50})

247   were listed in **Table 1**. The IC_{50} values for the seven compounds varied

248   for each cell line. A comparison of IC_{50} values showed that Umbelliprenin

249   (UM) and Lariciresinol (LA) were the most anti-proliferative compounds

250   against AGS gastric cancer cell line. In addition, UM and LA were less

251   cytotoxic to GES-1 cells compared with AGS cells (**Fig. 1b**). Therefore,

252   we chose UM and LA for further investigation.

253   Trypan blue dye exclusion was used to further evaluate the cytotoxicity of

254   the two compounds in AGS cells. Cells were exposed to various

255   concentrations of the two chemicals for 24 h. **Fig. 1c** showed the increase

256   of dead cells. Together, these data suggested that UM and LA can

257   preferentially inhibit the growth and induce the death of AGS cells while

258   being less cytotoxic to GES-1cells.

259

260   **The effects of UM and LA on morphological changes in AGS cells**

261   To elucidate whether UM and LA inhibited AGS cell growth by inducing

262   apoptosis, we used Hoechst 33342 and AO/EB staining to study the

263   number of apoptotic cells. Based on IC_{50} values, we chose 13.67 μM of

264   UM and 20.82 μM of LA and higher concentrations as treatments for

265   AGS cells. After Hoechst 33342 staining, typical morphological changes

266   of apoptosis such as condensed chromatin and apoptotic bodies were

267   observed when cells were exposed to both compounds (**Fig. 2a**). In

268   contrast, control cells exhibited round nuclei and chromatin were well

269   distributed. After AO/EB staining, apoptosis cells were observed as

270   orange nuclei (**Fig. 2b**). These observations indicated that the

271   proliferation inhibition effect of UM and LA may be related to apoptosis

272   induction.

273

274   **UM and LA induce apoptosis in AGS cells**

275   To further characterize the apoptosis process of AGS cells induced by

276   UM and LA, we assessed the numbers of apoptotic cells using Annexin

277   V-FITC/PI apoptosis staining. After 24 h exposure to UM, the population

278   of apoptotic cells (AV+/PI- plus AV+/PI+) increased in a dose-dependent

279   manner (**Fig. 3a**). The cellular apoptotic rates were lower when exposed

280   to LA (**Fig. 3b**). These results indicate that UM is more effective than LA

281   in the induction of apoptosis in AGS gastric cancer cells.

282

283   **UM and LA induce the decrease of mitochondrial membrane**

284   **potential (MMP) in AGS cells**

285   Apoptosis is also marked by the decrease of $\Delta\psi$ and JC-1 is often used as

286   an indicator to detect $\Delta\psi$ during apoptosis. The decrease of MMP was

287 measured as the increasing ratio of green-to-red fluorescence. As shown

288 in **Fig. 4**, JC-1 fluorescence mostly appeared in red in the control group

289 which indicated that the majority of cells were alive. UM treatment

290 induced a significant increase of green fluorescence which indicated the

291 loss of $\Delta\psi$. The fluorescence ratios after UM treatment were higher than

292 LA treatment, which indicated that apoptosis induction is associated with

293 the loss of $\Delta\psi$, with UM is more effective than LA.

294

295 **UM and LA affect the generation of ROS**

296 ROS production was evaluated by the level of hydrogen peroxide

297 production, using DCFH-DA detected by flow cytometry. After AGS cells

298 were treated with UM or LA for 24 h, ROS production, as indicated by

299 fluorescence, increased in a dose-dependent manner (**Fig. 5**). UM

300 treatment (13.67 μM) caused a remarkable increase of fluorescence

301 compared with control group; while the results of LA treatment showed

302 slower increase of fluorescence respectively. Together, these data showed

303 that both UM and LA could generate ROS in AGS cells, with UM being

304 more effective.

305

306 **Effects of UM and LA on apoptosis-related protein expression in**

307 **AGS gastric cancer cells**

308 The Bcl-2 protein family is the key regulator of apoptosis [13]. Our results

309   showed that UM and LA both induced apoptosis in AGS cells. We then

310   analyzed the protein expression of Bax and Bcl-2 after treating with UM

311   or LA. Western blot results showed an increase in the level of Bax and a

312   reduction of Bcl-2 protein after treatment with UM or LA (**Fig. 6a**).

313   Caspase-3 is an executioner which cleaves a broad spectrum of cellular

314   target proteins like nuclear PARP, leading to a cell death cascade. We

315   examined the activation of Caspase-3 and cleaved PARP after exposure to

316   UM or LA. The results showed a decrease in Cleaved PARP and an

317   increase in Cleaved Caspase-3 (**Fig. 6a**). Relative protein expression

318   results are shown in Fig. 6c. Combined with the JC-1 test, these results

319   indicated that the mitochondrial apoptotic pathway is activated by UM

320   and LA.

321

322   UM and LA increase G0/G1 arrest of cell cycle in AGS cells

323   As UM and LA showed significant growth inhibition and effective

324   apoptosis induction in AGS cells, we investigated their effects on cell

325   cycle. AGS were treated with UM or LA for 24 h, followed by flow

326   cytometry analyses. The UM-treated group showed G0/G1 phase arrest

327   compared with control groups (**Fig. 7a**). Similar results were obtained

328   when cells were treated with LA, with a slightly lower number of cells

329   arrested in G0/G1 phase compared with the UM groups (76.26 ± 2.06%

330   for UM and 71.61 ± 3.12% for LA) (**Fig. 7b**). The distribution of AGS

331 cells in cell cycle treated by UM or LA are shown in **Fig. 7c** and **Fig. 7d**,

332 indicating G0/G1 arrest in cell cycle. These results suggested that growth

333 inhibition and apoptosis induction of UM and LA in AGS gastric cancer

334 cells is at least partly associated with the induction of G0/G1 arrest in cell

335 cycle.

336

337 **Effects of UM and LA on cell cycle regulation-related protein**

338 **expression in AGS cells**

339 To gain a further understanding about the molecular mechanisms in AGS

340 cells during cell cycle arrest, we analyzed the effects of UM and LA on

341 the expression of some major regulatory proteins. **Fig. 6b** showed that

342 after treatment with UM or LA, the expression of cyclin D1, cyclin E,

343 CDK2 and CDK4 decreased, while the expression of P27, P16 and Rb

344 increased. Relative protein expression results are shown in Fig. 6d.These

345 results suggest that changes of protein expression may play important

346 roles in G0/G1 arrest of cell cycle in AGS cells.

347

348 **UM and LA inhibit tumor growth in BGC-823 tumor xenograft**

349 **models**

350 To assess the antitumor effects of UM and LA in xenograft models,

351 human gastric cancer cells BGC-823 were inoculated subcutaneously into

352 nude mice. Five groups of xenograft mice were administered with vehicle

353   (control), 10 mg/kg and 20 mg/kg of UM, 10 mg/kg and 20 mg/kg of LA

354   twice a day for 12 days and sacrificed at the end. The data showed that

355   tumors from both UM and LA treatment groups grew slowly than the

356   control group **(Fig. 8c and Fig. 8d)**. In detail, no significant difference of

357   the tumor volume in each group was observed at the beginning of

358   treatment. At the end of treatment, tumor inhibition rates of UM were

359   63.64% (20 mg/kg) or 40.81% (10 mg/kg) and 43.33% (20 mg/kg) or

360   37.24% (10 mg/kg) in LA treatment groups when compared to the control

361   group **(Fig. 8a)**. The body weights in treatment groups slightly decreased

362   during the treatment **(Fig. 8b).** Together, these data suggest that UM and

363   LA effectively inhibit tumor growth.

364

365   **Discussion**

366   Gastric cancer is one of the most common malignant diseases, and ranks

367   second in mortality among all cancers worldwide [14]. Currently,

368   chemotherapy is used as the primary treatment for this disorder. However,

369   overall survival rates of patients are low, while the incidences of side

370   effects are high [15]. Therefore, natural products with the potential for

371   gastric cancer treatment have gained a lot of attention. *F. sinkiangensis*

372   (called A-WEI in Mandarin) has been used as an effective medicine in

373   treating stomach disorders in Xinjiang District of China for thousands of

374   years [16]. In addition, there have been recent studies on the isolation of

375 compounds from the roots and volatile oil from *F. sinkiangensis* [10,17].

376 However, studies on the efficacy and mechanism of the anti-gastric

377 cancer effects of this valuable medicine have not been reported yet. Our

378 previous results showed that a petroleum ether extract from the seeds

379 exhibit antitumor effect *in vivo*. Based on these observations we

380 performed a further research on the compounds isolated from the seeds.

381 In the present study, we found seven compounds that show anti-gastric

382 cancer activity. After screening, we found UM and LA were the most

383 effective compounds in inhibiting the growth of AGS gastric cancer cells

384 among the seven compounds tested. We then took these two compounds

385 as potential therapeutic agents in gastric cancer treatment for further

386 study.

387 In this study, UM and LA showed the best antitumor activity against AGS

388 cells with lower toxicity against normal human gastric epithelial cells and

389 other cancer cell lines, suggesting that UM and LA could be both

390 effective and specific agents against human gastric cancer cells. Cell

391 selectivity related with multiple factors such as metabolism and

392 interaction with specific receptors and tumor microenvironment. There

393 have been researches on the relations between compounds and biological

394 targets in their selectivity for cancer cells. For example, a series of

395 6,7,10-trimethoxy-α-naphthoflavones (4a−o) were synthesized and their

396 inhibitory potency against cancer cells related with their selectivity for

397   CYP1B1 in human breast adenocarcinoma MCF-7 cell line [18]. And

398   purine-scaffold compound series showed cell selectivity for different

399   effects on Grp94 which could regulate intracellular trafficking of Toll-like

400   receptor 9 [19]. There has also been research on tumor microenvironment

401   showed that the inhibitory effect of iron chelator DIBI on human and

402   murine mammary carcinoma and fibrosarcoma cells varies for the change

403   of tumor microenvironment [20]. Besides these factors the inhibition of

404   cancer cell proliferation is often associated with cell cycle arrest [21]. The

405   G1 phase is a key part of the cell cycle. It is involved in the pathogenesis

406   of many diseases, and also the entry point for many drug therapies [22]. The

407   few reports on the effects of UM on cell cycle progression demonstrate

408   that UM arrests the growth of human M4Beu metastatic pigmented

409   malignant melanoma cells by G1 arrest [23], whereas no reports on the

410   effects of LA on cell cycle have been reported. Our results showed that

411   UM and LA arrest AGS cells in G0/G1 phase, which prevents the

412   conversion to the S phase and M phase, suggesting one possible

413   mechanism for cell cycle arrest by UM and LA. Western blot results

414   showed that cyclin D, cyclin E, CDK4 and CDK2 were down-regulated

415   after treatments, while CDK inhibitors p27, P16, and downstream Rb

416   were up-regulated. The CDK inhibitors have been shown to arrest the cell

417   cycle and inhibit the growth of cancer cells [24]. These results may

418   therefore provide an additional explanation for the G0/G1 phase arrest

419 induced by UM and LA.

420 Apoptosis induction plays an important role in the inhibition of tumor

421 cells [25]. Although UM and LA have been shown to induce apoptosis in

422 some cancer cells [23,26-28], the effects on anti-gastric cancer cells have not

423 been reported, and the mechanism is not fully understood. In the present

424 study, after AO/EB and Hoechst 33342 staining, AV/PI apoptosis

425 detection, and changes in MMP and ROS tests, we found that both UM

426 and LA can induce apoptosis in gastric cancer AGS cells. When the cells

427 were active in the apoptotic pathway, the signal caused the activation of

428 Caspase-3, which led to apoptosis [29,30]. Western blot analysis showed that

429 both UM and LA can activate Caspase-3, cleaving the substrate PARP at

430 the same time. We also found an increase in pro-apoptotic protein Bax

431 expression and a decrease in anti-apoptotic protein Bcl-2 expression in

432 AGS cells. An increase in the ratio of Bax/Bcl-2 stimulates the induction

433 of apoptosis [31]. These results support the roles of Caspase-3 and Bcl-2

434 family proteins in both UM and LA-induced apoptosis in gastric cancer

435 cells. The *in vivo* anticancer activity of UM and LA were evaluated in

436 human gastric cancer BGC-823 xenograft models. The results showed

437 that both UM and LA can reduce the volume of tumor *in vivo*.

438 Notably, although the IC_{50} values of UM and LA in cells varies, the

439 protein expression levels after treatment by the two compounds showed

440 no obvious differences. The effects of LA lag behind UM and could be a

441 contributing factor to these results. Thus, the mechanisms involving the

442 relationships between structure and function are not clear, and further

443 investigations are necessary.

444 In conclusion, we found UM and LA were the most specific and effective

445 compounds in the growth inhibition of human gastric cancer AGS cells

446 among the seven compounds which were first isolated from the seed of *F.*

447 *sinkiangensis K. M. Shen*. UM and LA could induce apoptosis in AGS

448 cells with increased Bax/Bcl-2 ratios, the generation of ROS, and the

449 decrease of MMP. UM and LA could also induce G0/G1 phase arrest in

450 cell cycle through the regulation of the G0/G1 phase checkpoint proteins.

451 Therefore, UM and LA could be treated as valuable candidates for further

452 investigation as possible antitumor treatments for gastric cancer.

453

462

References

463

464 1 Y. J. Yu, W. J. Sun, M. D. Lu, F. H. Wang, D. S. Qi, Y. Zhang, P. H. Li, H. Huang, T. You
465 and Z. Q. Zheng, *World J Gastroentero.,* 2014, **20**, 18413-18419.

466 2 R. Siegel, J. Ma, Z. Zou and A. Jemal, *CA-Cancer J Clin.,* 2014, **64**, 9-29.

467 3 C. Pinto, F. Fabio, S. Siena, S. Casxinu, L. F. L. Rojas, C. Ceccarelli, V. Mutri, L.
468 Giannetta, S, Giaquinta, C. Funaioli, R. Berardi, C. Longobardi, E. Piana and A. A.
469 Martoni, *Ann oncol.,* 2007, **18**, 510-517 (2007).

470 4 V. E. Cutsem, *Proc ASCO.,* 2009, **ABSTRACT**, LBA4509.

471 5 F. H.Cortés, F. Rivera, I. Alés, A. Márquez, A. Velasco, R. Colomer, C. R. Garcia, J.
472 Sastre, J. Guerra and C. Gravalos, *Ann oncol.,* 2007, **25**, 4613.

473 6 R. Qin, H. Shen, Y. Cao, Y. Fang, H. Li, Q, Chen and W. Xu, *PloS one,* 2013, **8**, e76486.

474 7 M. Y. Xu, D. H. Lee, E. J. Joo, K. H. Son and Y. S, *Food chem toxicol.,* 2013, **59**,
475 703-708.

476 8 S. He, and D. Y. Tan, *J Xinjiang Agr Univ.,* 2005, **25**, 1-7.

477 9 H. Zhang, and J. Hu, *Chin Pharmacol Bull.,* 1987, **3**, 288-290.

478 10 J. R. Yang, Z. An, Z. H. Li, S. Jing and H. L. Qina, *Chem Pharm bull.,* 2006, **54**,
479 1595-1598.

480 11 G. Z. Li, X. J. Li, L. Cao, L. G. Shen, J. Zhu, J. Zhang, J. C. Wang, L. J. Zhang and J. Y.
481 Si, *Fitoterapia,* 2014, **97**, 247-252.

482 12 Y. E. Wang, J. Y. Si, X. J. Li, L. Jiang and J. Zhu, *Mod Chin Med.,* 2011, **13**, 26-28.

483 13 W. A. Siddiqui, A. Ahad and H. Ahsan, *Arch Toxicol.,* 2015, **89**, 289-317.

484 14 M. B. Piazuelo and P. Correa, *Colombia Médica,* 2013, **44**, 192-201.

485 15 X. Paoletti, K. Oba, T. Burzykowski, S. Michiels, Y. Ohashi, J. P. Pignon, P. Rougier, J.
486 Sakamoto, D. Sargent, M. Sasako, E. Van Cutsem and M. Buyse, *Jama,* 2010, **303**,
487 1729-1737.

488 16 C. Tian, L. Q. Xie and G. LI, *Seed,* 2008, **5**, 88-90.

489 17 B. Ye, S. Wang and L. Zhang, *Nat Prod Res.,* 2011, **25**, 1161-1170.

490 18 J. H. Zhang, Q. Q. Meng, X. Zhang, Q. Cui, W. Zhou and S. S. Li, *J Med. Chem.,* 2015,
491 **58**, 3534-3547.

492 19 H. J. Patel, P. D. Patel, S. O. Ochiana, P. R. Yan, W. L. Sun, M. R. Patel, S. K. Shah, E.
493 Tramentozzi, J. Brooks, A. Bolaender, L. Shrestha, R. Stephani, P. Finotti, C. Leifer, Z. H.
494 Li, D. T. Gewirth, T. Taldone and G. Chiosis, *J Med. Chem.,* 2015, **58**, 3922-3943.

495 20 M. R. P. Coombs, T. Grant, A. L. Greenshields, D. J. Arsenault, B. E. Holbein and D. W.
496 Hoskin, *Exp Mol Pathol.,* 2015, **99**, 262-270.

497 21 R. Marcotte and E. Wang, *J Gerontol.,* 2002, **57**, B257-269.

498 22 M. Narita, S. Nunez, E. Heard, M. Narita, A. W. Lin, S. A. Hearn, D. L. Spector,G. J.
499 Hannon and S. W. Lowe, *Cell,* 2003, **113**, 703-716.

500 23 C. Barthomeuf, S. Lim, M. Iranshahi and P. Chollet, *Phytomedicine,* 2008, **15**, 103-111.

501 24 M. Malumbres and M. Barbacid, *Nat Rev: Cancer.,* 2009, **9**, 153-166.

502 25 S. W. Lowe and A. W. Lin, *Carcinogenesis,* 2000, **21**, 485-495.

503 26 N. Khaghanzadeh, Z. Mojtahedi, M. Ramezani, N. Erfani and A. Ghaderi, *Daru,* 2012, **20**,
504 69-74.

505 27 S. A. Ziai, O. Gholami, M. Iranshahi, A. H. Zamani and M. Jeddi-Tehrani, *Iran J Pharm*

22

506   *Res.,* 2012, **11**, 653-659.

507   28   F. Bakar, M. G. Caglayan, F. Onur, S. Nebioglu, S and I. M. Palabiyik, *Anti-cancer Agent*
508   *Med.,* 2014, **15**, 336-344.

509   29   N. N. Danial, *Clin Cancer Res.,* 2007, **13**, 7254-7263.

510   30   T. T. Huang, S. P. Wu, K. Y. Chong, D. M. Ojcius, Y. F. Ko, Y. H. Wu, C. Y. Wu, C. C. Lu,
511   J. Martel, J. D. Young and H. C. Lai, *J Ethnopharmacol.,* 2014, **155**, 154-164.

512   31   J. Han, P. Tan, Z. Li, Y. Wu, C. Li, Y. Wang, B. Wang, S. Zhao and Y. Liu, *PloS one,* 2014,
513   **9**, e86539.

514   **Figure Legends**

515   Fig. 1. Active compounds and inhibition effects on cell viability.

516   Chemical structures of seven active compounds isolated from the seed of

517   *Ferula sinkiangensis* (**Fig. 1a**). Effects of UM and LA on the viabilities of

518   human AGS gastric cancer cells AGS (**Fig. 1b**) and human normal gastric

519   epithelial cells GES-1 (**Fig. 1c**). AGS and GES-1 were exposed to various

520   concentrations of the compounds (0, 6.25, 12.5, 25, 50, 100 μM) for 24 h

521   or   48   h,   followed   by   the   3-(4,5-dimethylthiazol-2-yl)-2,

522   5-diphenyltetrazolium bromide (MTT) assay. UM and LA suppressed cell

523   viability and induced AGS cells death, while being less cytotoxic to

524   GES-1cells. The cytotoxic effects of UM and LA on AGS cells was also

525   determined by trypan blue dye exclusion (**Fig. 1d**). The data represent the

526   mean value of three independent experiments and are expressed as means

527   ± SD. [**]P < 0.01 was considered statistically significant.

528

529   Fig. 2. Induction of apoptosis by UM and LA in AGS cells. Micrographs

530   show apoptotic cells after treatment with UM or LA at different

531   concentrations and staining by Hoechst 33342 for 24 h (**Fig. 2a**).

532 Micrographs show apoptotic cells treated by UM or LA for 24 h at

533 different concentrations, followed by staining with AO/EB (**Fig. 2b**).

534

535 Fig. 3. UM and LA induced apoptosis in AGS cells detected by the

536 Annexin V-FITC/PI staining test.

537 AGS cells were treated with UM (0, 13.67, 27.34, 54.58 μM) (**Fig. 3a**,

538 **Fig. 3b**) or LA (0, 20.82, 41.62, 83.24 μM) (**Fig. 3c**, **Fig. 3d**) for 24 h.

539 DMSO treatment was used as a vehicle control. The apoptotic rates were

540 determined by Annexin V-FITC/PI staining. Dot-plot graphs show viable

541 cells (AV-/PI-), necrotic cells (AV-/PI+), early phase apoptotic cells

542 (AV+/PI-), and late phase apoptotic cells (AV+/PI+). $^*P < 0.05$ and $^{**}P <$

543 0.01 were considered statistically significance.

544

545 Fig. 4. UM and LA induced mitochondrial membrane potential (MMP)

546 depolarization in AGS cells.

547 AGS cells were cultured in UM (0, 13.67, 27.34, 54.58 μM) (**Fig. 4a**, **Fig.**

548 **4b**) or LA (0, 20.82, 41.62, 83.24 μM) (**Fig. 4c**, **Fig. 4d**) for 24 h. DMSO

549 treatment was used as vehicle control. Cells were then labeled with JC-1

550 and analyzed by flow cytometry. Results obtained from a representative

551 experiment are shown (n=3). Statistical significance was $^{**}P < 0.01$.

552

553 Fig. 5. Effects of UM and LA on the generation of reactive oxygen

554   species (ROS).

555   AGS gastric cancer cells were treated with UM or LA for 24 h. The

556   increasing level of intracellular ROS after treatment of AGS cells was

557   measured by flow cytometry after staining with DCFDA (**Fig. 5**). Data

558   are expressed as percentage of green signals. [*]$P < 0.05$ and [**] $p<0.01$ were

559   considered statistically significant.

560

561   Fig. 6. The effects of UM and LA on the expression of apoptosis-related

562   proteins (**Fig. 6a** and **Fig. 6c**) and cell cycle-related proteins (**Fig. 6b** and

563   **Fig. 6d**) were determined by western blot.

564   AGS cells were treated with UM (0, 13.67, 27.34, and 54.58 μM) or LA

565   (0, 20.82, 41.62, and 83.24 μM) for 24 h. UM and LA decreased the

566   expression of Bcl-2 and cleaved PARP, and increased the expression of

567   Bax   and   cleaved   Caspase-3.   Relative   expression   levels   of

568   apoptosis-related proteins and cell cycle-related proteins are showed in

569   **Fig. 6c** and **Fig. 6d**. β-actin was used to confirm equal protein loading.

570   UM and LA decreased the expression of cyclin D1, cyclin E, CDK2 and

571   CDK 4, with the expression of P27, P16 and Rb increased. β-actin was

572   used to confirm equal protein loading. [*]$P < 0.05$ and [**] $p<0.01$ were

573   considered statistically significant.

574

575   Fig. 7. Effects of UM and LA on cell cycle progression in AGS cells.

576 Cells were treated by UM (0, 13.67, 27.34, 54.58 μM) (**Fig. 7b**) or LA (0,

577 20.82, 41.62, 83.24 μM) (**Fig. 7d**) for 24 h and then analyzed by flow

578 cytometry for cell cycle distribution. Cell cycle distributions after UM

579 (**Fig. 7a**) or LA (**Fig. 7c**) treatment in AGS cells are shown. All tests were

580 done in triplicate. [*] $P < 0.05$ when compared with the control group.

581

582 Fig. 8. Anti-tumor effects of UM and LA in BGC-823 xenograft tumor

583 models. UM and LA could inhibit tumor growth in BGC-823 xenograft

584 models. **Fig. 8a** was the picture of the excised tumors on day 12 in UM

585 and LA treatment groups. **Fig. 8b** showed the body weight curves of

586 xenograft mice in UM and LA treatment groups. **Fig. 8c** and **Fig. 8d**

587 showed the tumor volume growth curve of xenograft models in UM and

588 LA treatment groups. *$P < 0.05$ compared with control mice.

589

590 **Contributions**

591 L.C. and X.S. designed the experiments; X.L. identified the plant material;

592 J.Y. and G.Z. isolated compounds. Li.Z., Le.Z., L.G., X.H. and D.L.

593 performed the experiments; Li.Z. analyzed the data and wrote the

594 manuscript. All authors reviewed the manuscript and approved it for

595 submission.

596

597 **Competing financial interests**

598   The authors declare no competing financial interests.

599

600   Table 1

601   Cytotoxicity of compounds isolated from the seeds of *Ferula*

602   *sinkiangensis*.

603

Compounds	IC50(μM)[a]				
	GES-1	AGS	HeLa	A549	PC3
Umbelliprenin	109.17±2.07	13.67±1.73	75.83±2.66	121.53±4.41	88.27±3.76
Lariciresinol	91.98±1.65	20.82±2.86	91.36±4.24	71.28±2.48	104.69±3.45
Quercetin	44.51±2.29	37.62±2.23	25.05±2.65	52.54±1.59	48.87±3.42
Macrathoin F	62.78±1.01	68.31±1.55	119.31±3.73	77.35±1.72	95.69±4.12
Arctigenin	67.82±1.86	87.76±3.67	65.23±1.86	102.58±3.93	54.43±1.91
(7,8-cis-8,8'-trans)-2' ,4'dihydroxyl-3,5-di methoxy-lariciresinol	112.92±3.51	89.01±3.14	152.84±1.83	167.29±4.22	118.68±4.83
Lehmannolol	79.53±2.97	156.76±3.78	182.38±4.75	>200	187.11±4.91

604

605   [a] IC_{50} is the concentration of compound causing 50% growth inhibition

606   for each cell line. The results represent the mean values of three

607   independent tests.
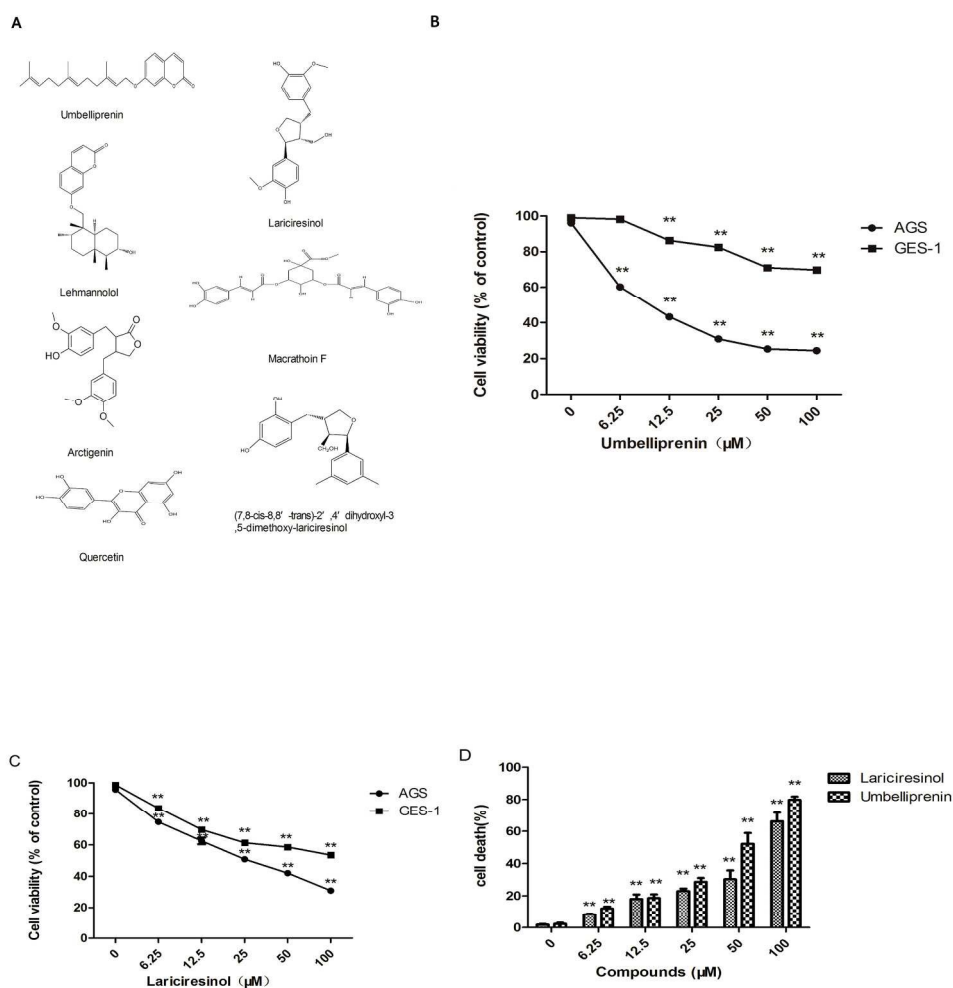
Fig. 1. Active compounds and inhibition effects on cell viability.
Chemical structures of seven active compounds isolated from the seed of Ferula sinkiangensis (Fig. 1a).
Effects of UM and LA on the viabilities of human AGS gastric cancer cells AGS (Fig. 1b) and human normal
gastric epithelial cells GES-1 (Fig. 1c). AGS and GES-1 were exposed to various concentrations of the
compounds (0, 6.25, 12.5, 25, 50, 100 μM) for 24 h or 48 h, followed by the 3-(4,5-dimethylthiazol-2-yl)-2,
5-diphenyltetrazolium bromide (MTT) assay. UM and LA suppressed cell viability and induced AGS cells
death, while being less cytotoxic to GES-1cells. The cytotoxic effects of UM and LA on AGS cells was also
determined by trypan blue dye exclusion (Fig. 1d). The data represent the mean value of three independent
experiments and are expressed as means ± SD. **$P < 0.01$ was considered statistically significant.

219x225mm (300 x 300 DPI)

A

B
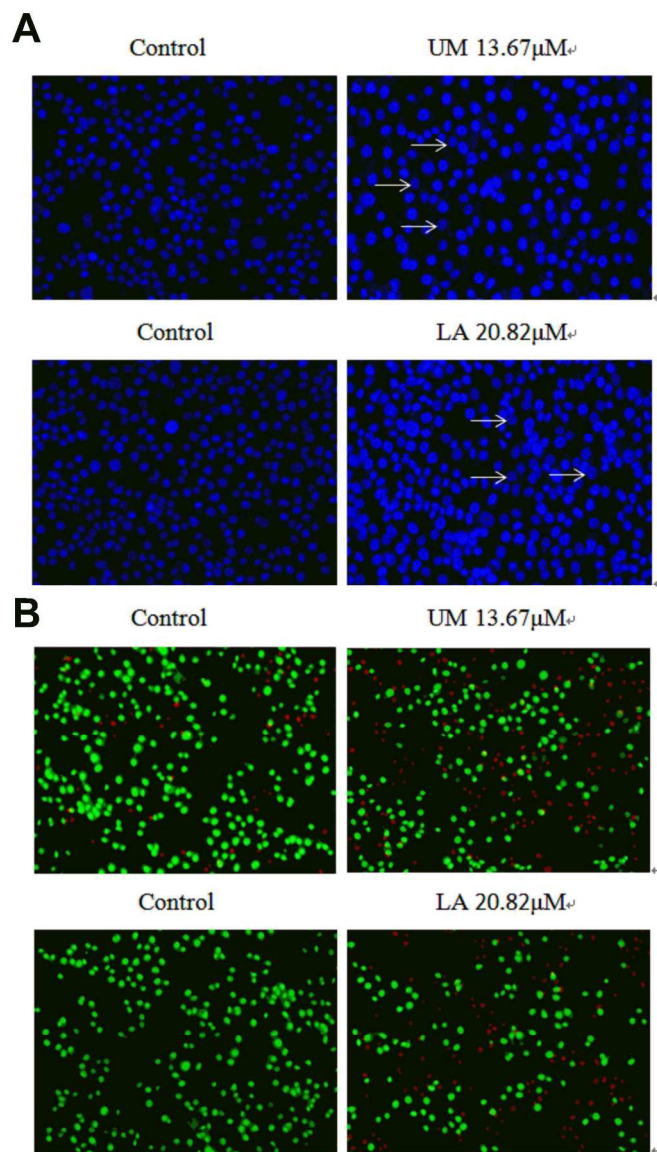
210x366mm (300 x 300 DPI)
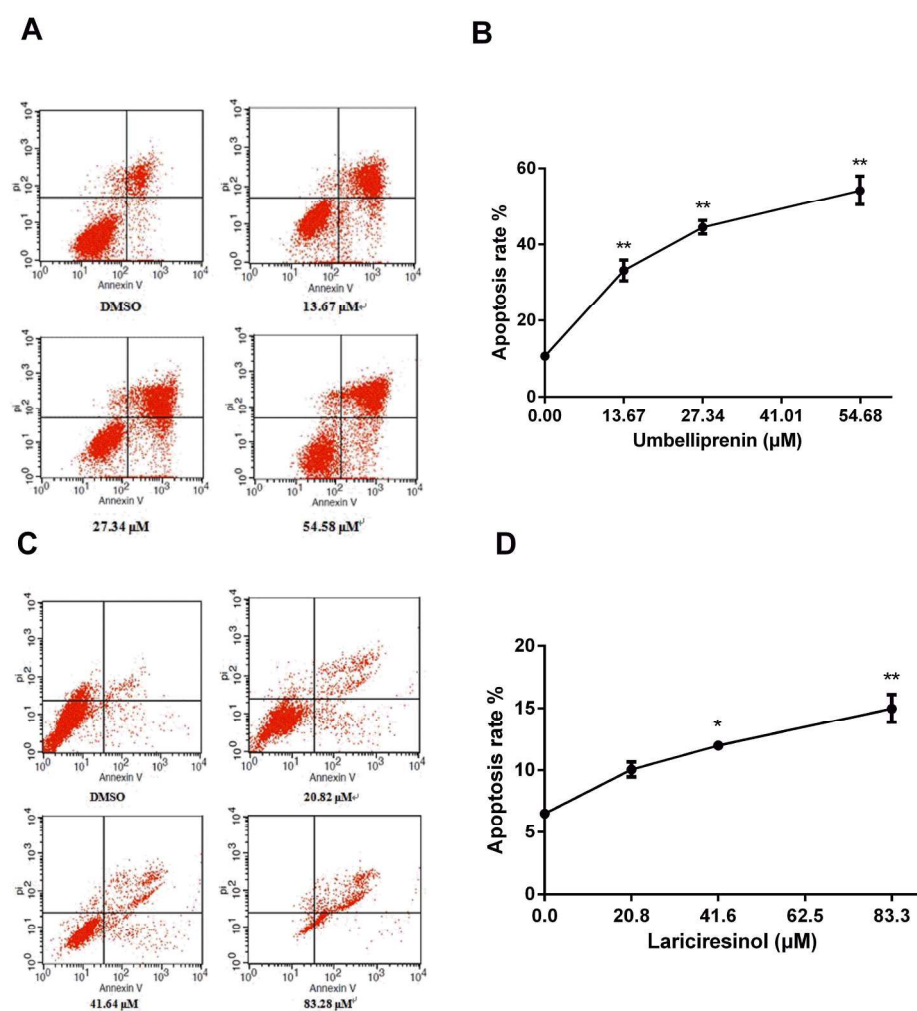
Fig. 3. UM and LA induced apoptosis in AGS cells detected by the Annexin V-FITC/PI staining test. AGS cells were treated with UM (0, 13.67, 27.34, 54.58 μM) (Fig. 3a, Fig. 3b) or LA (0, 20.82, 41.62, 83.24 μM) (Fig. 3c, Fig. 3d) for 24 h. DMSO treatment was used as a vehicle control. The apoptotic rates were determined by Annexin V-FITC/PI staining. Dot-plot graphs show viable cells (AV-/PI-), necrotic cells (AV-/PI+), early phase apoptotic cells (AV+/PI-), and late phase apoptotic cells (AV+/PI+). *P < 0.05 and **P < 0.01 were considered statistically significance.

216x224mm (300 x 300 DPI)

A

DMSO

13.67 µM

27.34 µM

54.68 µM

B

C

DMSO

20.82 µM

41.64 µM

83.28 µM

D
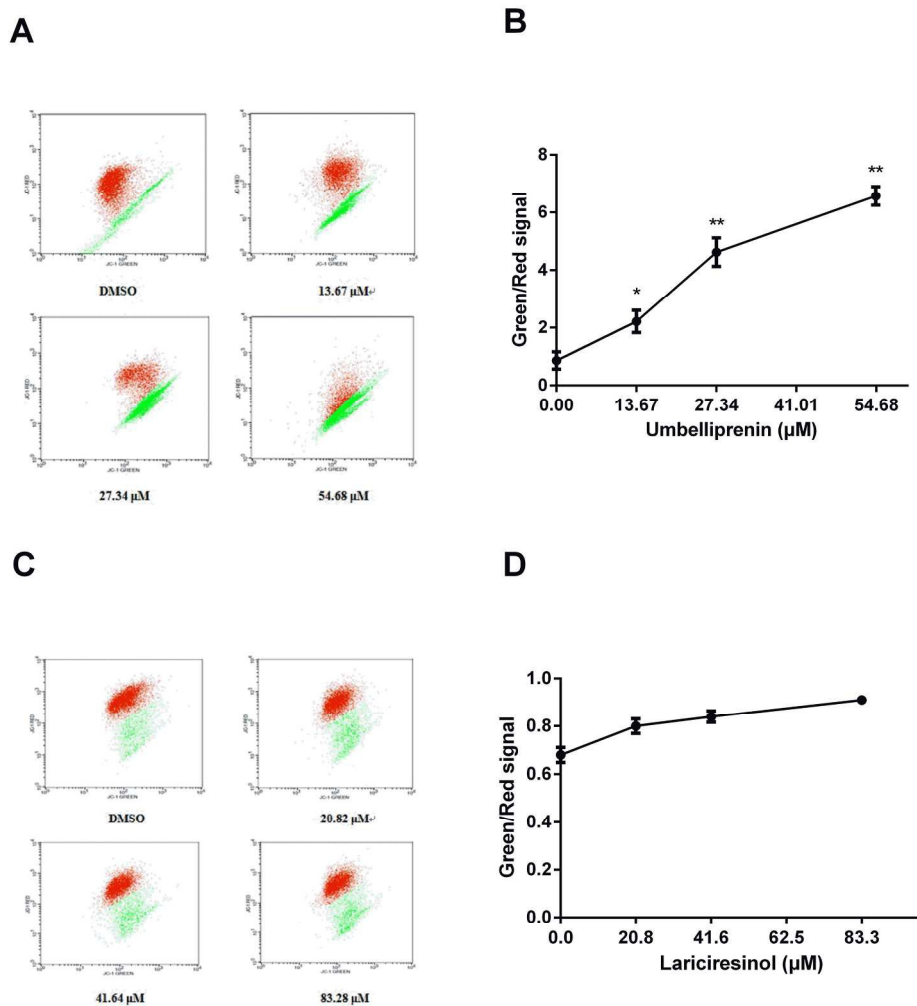
Fig. 4. UM and LA induced mitochondrial membrane potential (MMP) depolarization in AGS cells. AGS cells were cultured in UM (0, 13.67, 27.34, 54.58 µM) (Fig. 4a, Fig. 4b) or LA (0, 20.82, 41.62, 83.24 µM) (Fig. 4c, Fig. 4d) for 24 h. DMSO treatment was used as vehicle control. Cells were then labeled with JC-1 and analyzed by flow cytometry. Results obtained from a representative experiment are shown (n=3). Statistical significance was **P < 0.01.

220x229mm (300 x 300 DPI)
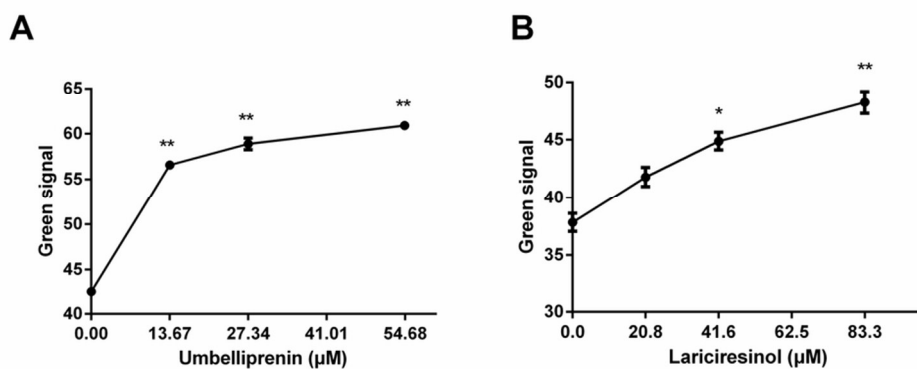
Fig. 5. Effects of UM and LA on the generation of reactive oxygen species (ROS).
AGS gastric cancer cells were treated with UM or LA for 24 h. The increasing level of intracellular ROS after treatment of AGS cells was measured by flow cytometry after staining with DCFDA (Fig. 5). Data are expressed as percentage of green signals. *P < 0.05 and ** p<0.01 were considered statistically significant.

86x35mm (300 x 300 DPI)
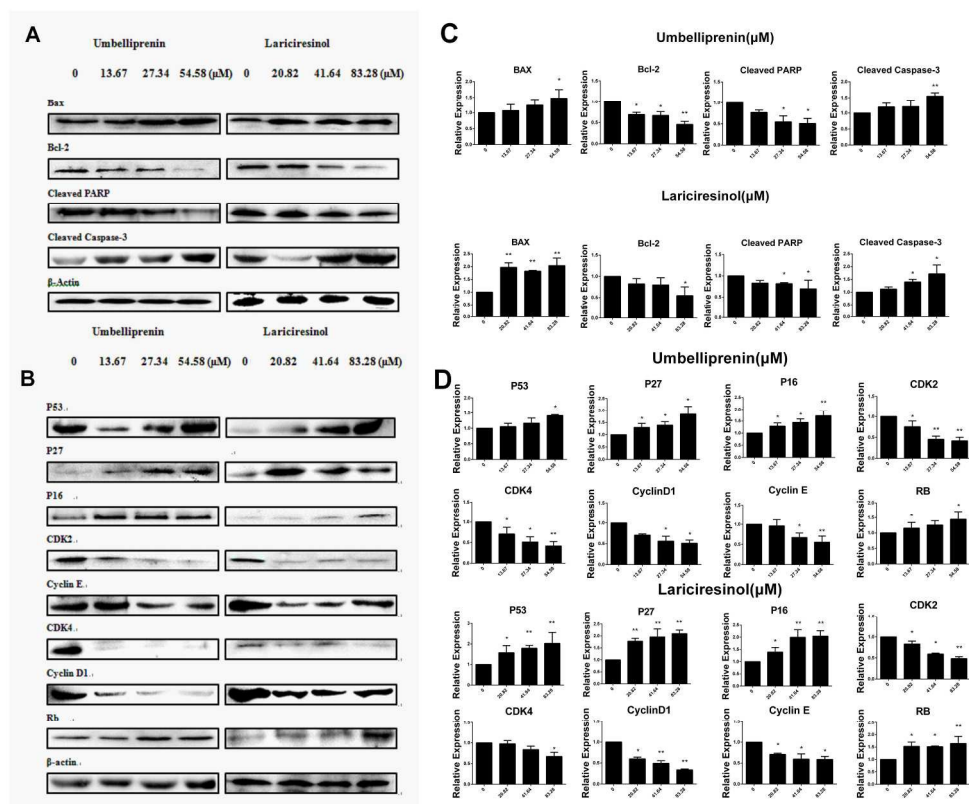
Fig. 6. The effects of UM and LA on the expression of apoptosis-related proteins (Fig. 6a and Fig. 6c) and cell cycle-related proteins (Fig. 6b and Fig. 6d) were determined by western blot.
AGS cells were treated with UM (0, 13.67, 27.34, and 54.58 µM) or LA (0, 20.82, 41.62, and 83.24 µM) for 24 h. UM and LA decreased the expression of Bcl-2 and cleaved PARP, and increased the expression of Bax and cleaved Caspase-3. Relative expression levels of apoptosis-related proteins and cell cycle-related proteins are showed in Fig. 6c and Fig. 6d. β-actin was used to confirm equal protein loading. UM and LA decreased the expression of cyclin D1, cyclin E, CDK2 and CDK 4, with the expression of P27, P16 and Rb increased. β-actin was used to confirm equal protein loading. *P < 0.05 and ** p<0.01 were considered statistically significant.

220x182mm (300 x 300 DPI)
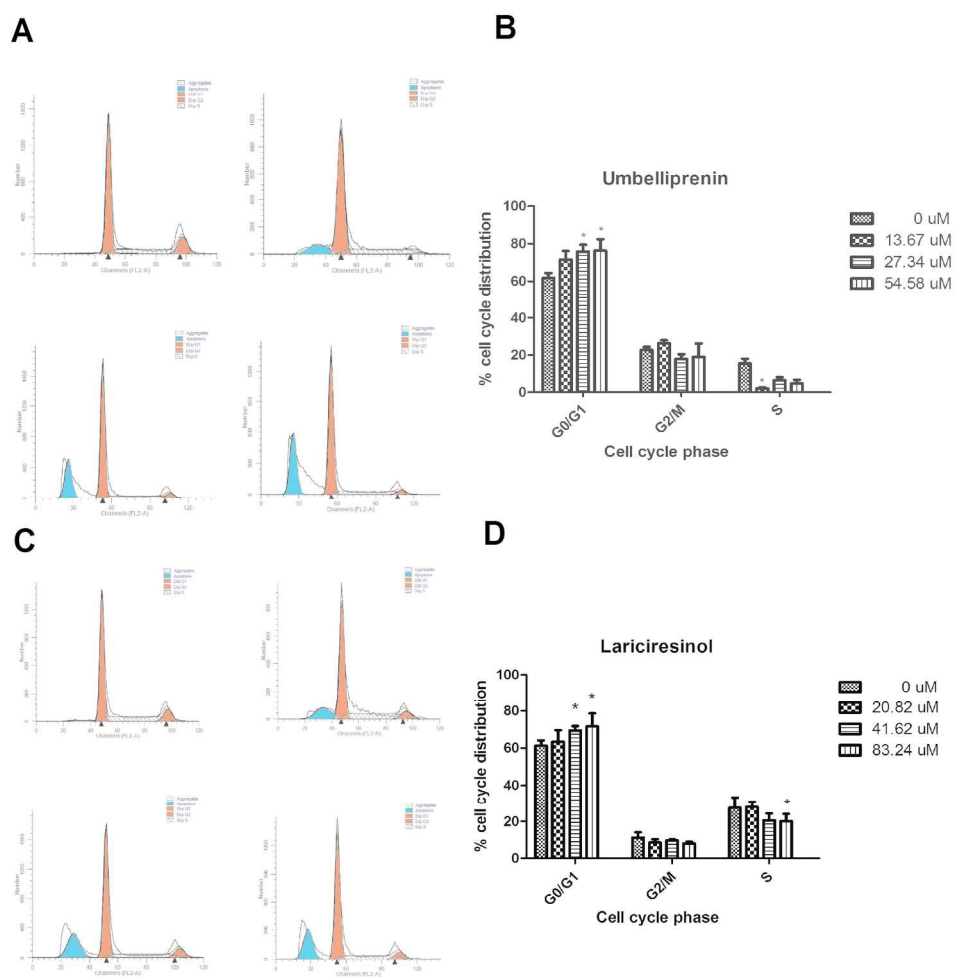
Fig. 7. Effects of UM and LA on cell cycle progression in AGS cells. Cells were treated by UM (0, 13.67, 27.34, 54.58 μM) (Fig. 7b) or LA (0, 20.82, 41.62, 83.24 μM) (Fig. 7d) for 24 h and then analyzed by flow cytometry for cell cycle distribution. Cell cycle distributions after UM (Fig. 7a) or LA (Fig. 7c) treatment in AGS cells are shown. All tests were done in triplicate. * P < 0.05 when compared with the control group. 218x221mm (300 x 300 DPI)
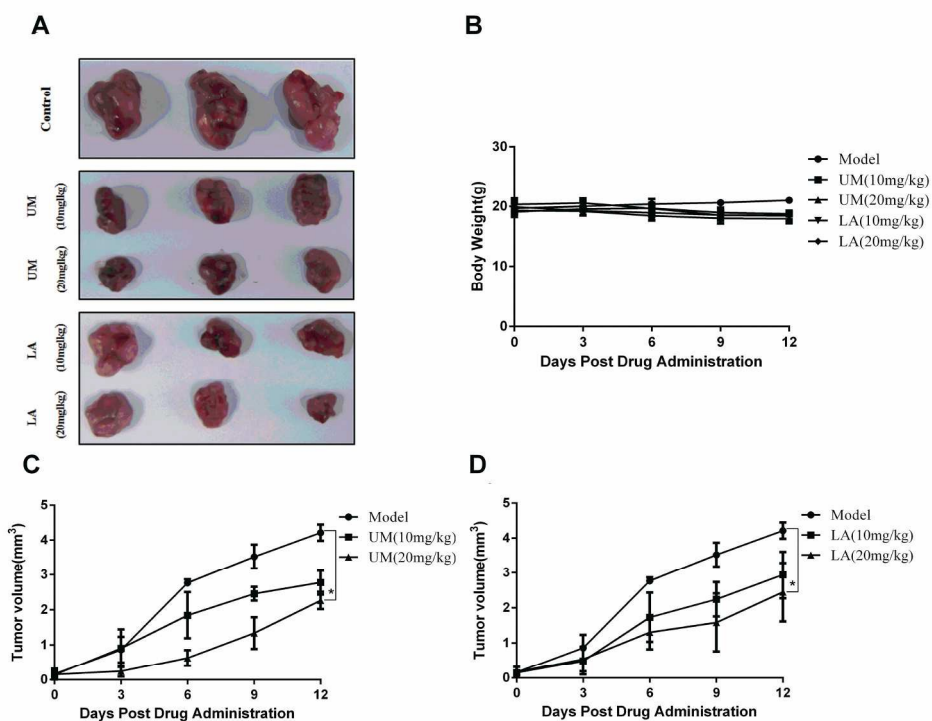
Fig. 8. Anti-tumor effects of UM and LA in BGC-823 xenograft tumor models. UM and LA could inhibit tumor growth in BGC-823 xenograft models. Fig. 8a was the picture of the excised tumors on day 12 in UM and LA treatment groups. Fig. 8b showed the body weight curves of xenograft mice in UM and LA treatment groups. Fig. 8c and Fig. 8d showed the tumor volume growth curve of xenograft models in UM and LA treatment groups. *P < 0.05 compared with control mice.
212x162mm (300 x 300 DPI)